

# Dominant Axis Theorem and the Area Preserving Lozi Map

Yoshihiro Yamaguchi<sup>1\*</sup> and Kiyotaka Tanikawa<sup>2</sup>

<sup>1</sup>Teikyo Heisei University, Ichihara, Chiba 290-0193, Japan

<sup>2</sup>National Astronomical Observatory, Mitaka, Tokyo 181-8588, Japan

\*E-mail address: chaosfractal@iCloud.com

(Received June 19, 2017; Accepted September 23, 2017)

In the family of the area preserving Hénon maps (the Hénon maps), the mapping function is quadratic. Replacing the quadratic function with a piecewise linear function, we obtain the area preserving Lozi map (the Lozi map). For the Hénon map, the elliptic periodic orbits appearing through rotation bifurcation of the elliptic fixed point have one orbital point on the particular axis, i.e., the dominant axis. Thus, the dominant axis theorem holds for the Hénon map. For the Lozi map, the dominant axis theorem does not hold. We make clear the reasons from the study of bifurcations. For the Lozi map, a new theorem instead of the dominant axis theorem is obtained.

**Key words:** Hénon Map, Lozi Map, Symmetric Periodic Orbit, Symmetry Axis, Dominant Axis Theorem

## 1. Introduction

Greene (Greene, 1979), in the standard map, took a branch of the symmetry axes and called it the dominant axis. He found numerically that particular symmetric elliptic orbits have one of the orbital points on the dominant axis. Since then, the result is called the dominant axis hypothesis. The hypothesis has been confirmed to be true in the standard map (MacKay and Meiss, 1983). Recently, it has been shown to be true in other mapping systems such as the connecting map (Dulling *et al.*, 2005; Yamaguchi and Tanikawa, 2016). In the present paper, we will show that the dominant axis theorem does not hold for the Lozi map (Lozi, 1978; Elhadj, 2013) in some parameter ranges by studying the bifurcations. We give a new theorem instead of the dominant axis theorem. In doing this, we develop a new geometrical method to determine the stability of the symmetric periodic orbits.

The dominant axis theorem is proper to reversible dynamical systems. So, we first introduce the reversible maps. We consider the area preserving map

$$T : y_{n+1} = y_n + f(x_n), \quad x_{n+1} = x_n + y_{n+1}, \quad (1)$$

with some function  $f(x)$ . For  $f(x) = f_H(x) = a(x - x^2)$  ( $a \geq 0$ ), we name  $T$  the connecting map included in the Hénon family (Hénon, 1976). Here the connecting map connects integrable and horseshoe maps (Yamaguchi and Tanikawa, 2016).

The map  $T$  is represented as  $T = h \circ g$ , where  $h \circ h = g \circ g = \text{id}$ , and  $\det \nabla h = \det \nabla g = -1$ . Two maps  $g$  and  $h$  are called the involutions. If, in general, a map is written as a product of involutions, the map is said to be reversible or to have reversibility in the sense of Birkhoff (Birkhoff,

1966). Here,  $g$  and  $h$  have the following concrete form.

$$g \begin{pmatrix} x \\ y \end{pmatrix} = \begin{pmatrix} x \\ -y - f(x) \end{pmatrix}, \quad h \begin{pmatrix} x \\ y \end{pmatrix} = \begin{pmatrix} x - y \\ -y \end{pmatrix}. \quad (2)$$

The set of the fixed points of involution is the symmetry axis. Let  $S_g$  and  $S_h$  be the symmetry axes of involutions  $g$  and  $h$ .

Here, we define symmetric periodic orbits and introduce the dominant axis theorem.

**Definition 1 (Symmetric periodic orbit).** The symmetric periodic orbit has two orbital points on the symmetry axes.

Let  $p/q$  be an irreducible fraction satisfying the conditions  $0 < p/q \leq 1/2$ . In the following theorem,  $p/q$ -BE and  $p/q$ -BS are monotone symmetric periodic orbits of rotation number  $p/q$ . These will be introduced in Subsec. 2.1.

**Theorem 2 (Dominant axis theorem).** For the Hénon map, a  $p/q$ -BE has one orbital point on the dominant axis  $S_g^+$  (see Fig. 1 and Eq. (4)) at  $a > a_c(p/q)$ . Therefore,  $p/q$ -BE's for all  $p/q$  have one of their orbital points on the dominant axis  $S_g^+$  at  $a > a_c(1/2)$ .

Theorem 2 implies that  $p/q$ -BS does not have its orbital point on  $S_g^+$  because orbital points of the  $p/q$ -BE and  $p/q$ -BS alternately surround fixed point  $Q$ . This is a strong restriction for  $p/q$ -BS.

Here, we give remarks for Theorem 2. In the standard map, once  $a$  becomes positive,  $p/q$ -BE of every rational number  $p/q$  appears and it has one orbital point on the dominant axis. On the other hand,  $p/q$ -BE appears through the rotation bifurcation of  $Q$  in the connecting map. Therefore, the condition for  $a$  is needed in Theorem 2. For the connecting map,  $a_c(1/2) = 4$  holds.

The dominant axis theorem plays an important role in

various occasions such as the study of disintegration of the invariant curves (Greene, 1979), structure of the intersection of the stable and unstable manifolds of the saddle fixed point (Yamaguchi and Tanikawa, 2001), and construction of the resonance regions (Yamaguchi and Tanikawa, 2009).

In the present paper, we take  $f(x) = f_L(x) = (a/2)(1 - |2x-1|)$  for  $a \geq 0$ . This is called the Lozi map (Lozi, 1978). The map is a piecewise linear version of the connecting map with  $f(x) = f_H(x)$ . For  $a > 0$ , we have  $f_L(0) = f_L(1) = f_H(0) = f_H(1) = 0$ . We also have  $f'_L(0) = f'_H(0) = a$  and  $f'_L(1) = f'_H(1) = -a$ , where the prime denotes the differentiation with respect to the argument, and  $f'(0)$ , say, is the slope of function  $f(x)$  at  $x = 0$ . The connecting maps and Lozi maps have fixed points  $P = (0, 0)$  and  $Q = (1, 0)$  for  $a > 0$ .

The fixed point  $P$  is a saddle with eigenvalues  $\lambda_{\pm}$  where  $0 < \lambda_- < 1 < \lambda_+$ . For  $0 < a < 4$ ,  $Q$  is an elliptic fixed point with complex eigenvalues. At  $a = 4$ ,  $Q$  undergoes period doubling bifurcation. At  $a > 4$ ,  $Q$  is a saddle with reflection with eigenvalues  $\lambda_- < -1 < \lambda_+ < 0$ .

The Smale horseshoe exists at  $a \geq 5.176605 \dots$  (Yamaguchi and Tanikawa, 2009) for the connecting maps, while at  $a \geq a_c^{\text{SH}} = 4.229981 \dots$  for the Lozi map. In the Lozi map, the mapping function  $f_L(x)$  has a break point at  $x = 1/2$ . As a result, the stable manifold  $W_s$  and the unstable manifold  $W_u$  of  $P$  have the break points (see Fig. 1). Using the break point, the critical value  $a_c^{\text{SH}}$  is determined analytically (see Appendix A).

The properties of the horseshoe are discussed in Guckenheimer and Holmes (1983), Gilmore and Lefranc (2002), and Yamaguchi and Tanikawa (2016).

Section 2 is for preparations. We summarize the bifurcations used in this paper and define the dominant axis for  $T^q$  for  $q \geq 1$ . In Sec. 3, we study the bifurcations in the Lozi map. It is shown that the dominant axis theorem does not hold for the Lozi map. In Sec. 4, a new theorem is obtained. In Sec. 5, we give concluding remarks.

## 2. Mathematical Tools

### 2.1 Bifurcations

We explain several known terms used in this paper. If the eigenvalues of the linearized matrix are complex, we call the corresponding periodic orbit “the elliptic periodic orbit with complex eigenvalues”. In the following argument the cases with  $\lambda = \pm 1$  are treated as those with complex eigenvalues for convenience.

If the eigenvalues satisfy relations  $\lambda_- < -1 < \lambda_+ < 0$ , we call the corresponding periodic orbit “the saddle periodic orbit with reflection”. The elliptic periodic orbit with complex eigenvalues and the saddle periodic orbit with reflection will together be called “elliptic” in the present report. If the eigenvalues satisfy relations  $0 < \lambda_- < 1 < \lambda_+$ , we call this periodic orbit a “saddle” as usual.

In this paper, we use the three bifurcations named rotation bifurcation, period doubling bifurcation and equiperiod bifurcation. In the following, we summarize them.

(i) **Rotation bifurcation.** If the average rotation rate, i.e., rotation number, around elliptic fixed point  $Q$  becomes an irreducible fraction  $p/q$  satisfying the conditions  $0 <$

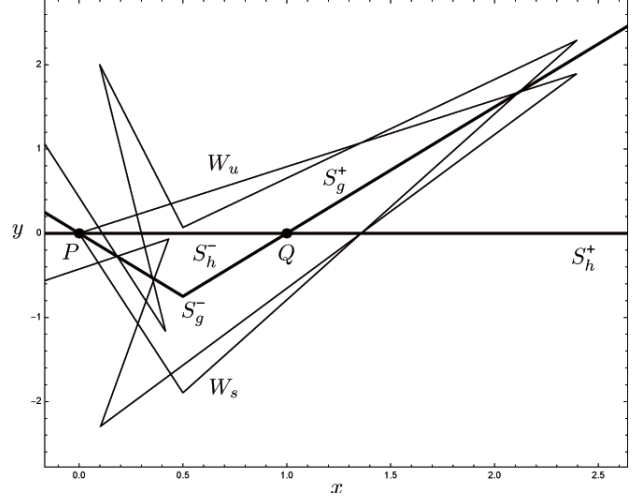


Fig. 1. The branches of symmetry axes  $S_g^+$ ,  $S_g^-$ ,  $S_h^+$ , and  $S_h^-$  are displayed at  $a = 3$ . The intersection points of symmetry axes are the fixed points  $P$  and  $Q$ . The stable manifold  $W_s$  and the unstable manifold  $W_u$  of the saddle fixed point  $P$  are also illustrated.

$p/q < 1/2$ , a pair of elliptic and saddle periodic orbits are born. We call this the rotation bifurcation of  $Q$ . Bifurcation parameter value is  $a = a_c(p/q) = 4 \sin^2(\pi p/q)$ . We denote the elliptic orbit by  $p/q$ -BE, and the saddle orbit by  $p/q$ -BS. Here, E in BE stands for “elliptic”, S in BS for “saddle”, and B in BE and BS for “Birkhoff”. The “Birkhoff” comes from mathematician’s name who studied the order-preservation property of orbits (Birkhoff, 1966). These are symmetric periodic orbits.

(ii) **Period doubling bifurcation.** The elliptic periodic orbit undergoes period doubling bifurcation if its eigenvalues arrive at  $\lambda = -1$  on the complex eigenvalue space. After period doubling bifurcation, the mother orbit becomes a saddle with reflection. A daughter periodic orbit with twice the period appears from the mother point and is elliptic with complex eigenvalues just after the appearance.

(iii) **Equiperiod bifurcation.** The elliptic periodic orbit undergoes equiperiod bifurcation if its eigenvalues arrive at  $\lambda = +1$  on the complex eigenvalue space. After the equiperiod bifurcation, the mother orbit becomes a saddle. Two daughter periodic orbits of the same period appear from the mother point and are elliptic with complex eigenvalues just after the appearance.

### 2.2 Involutions and symmetry axes for $T$

The Lozi map  $T$  is reversible. The set of the fixed points of involution is the symmetry axis. We give the representations of the symmetry axes  $S_g$  and  $S_h$ .

$$S_g : y = -f(x)/2, \quad S_h : y = 0. \quad (3)$$

Here, we also define the branches of symmetry axes.

$$S_g^+ : y = -f(x)/2 \quad (x \geq 1), \quad S_g^- : y = -f(x)/2 \quad (x < 1). \quad (4)$$

$$S_h^+ : y = 0 \quad (x \geq 1), \quad S_h^- : y = 0 \quad (x < 1). \quad (5)$$

Here,  $S_g^+$  is conventionally called the dominant axis (Dulling *et al.*, 2005). The symmetry axes and the stable and unstable manifolds of  $P$  are displayed in Fig. 1.

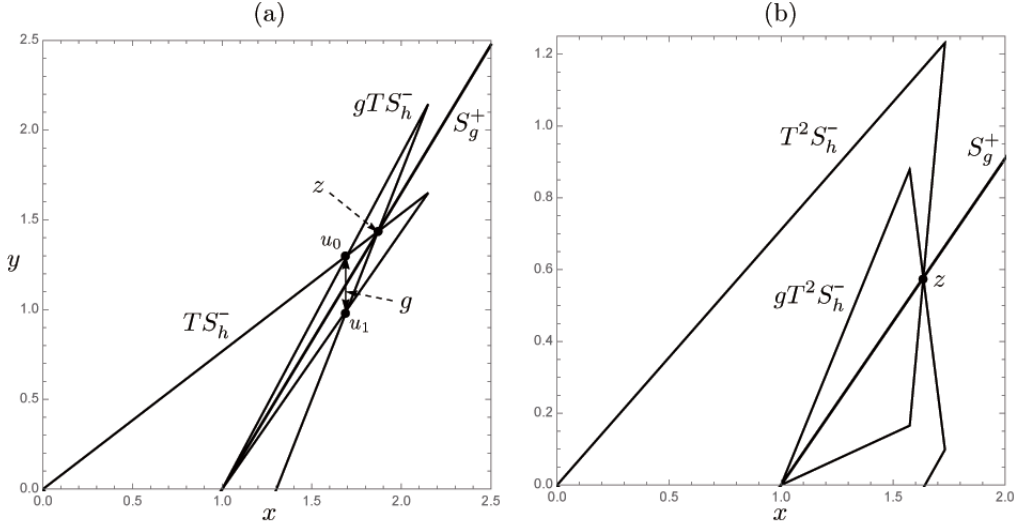


Fig. 2. (a) This figure represents the relation between the subdominant axis  $TS_h^-$  and its image  $gTS_h^-$  at  $a = 3.3 > a_c(1/3) = 3$ . The intersection point  $z$  is an orbital point of  $1/3$ -BE. The relation  $u_1 = gu_0$  holds. (b) This figure represents the relation between the subdominant axis  $T^2S_h^-$  and its image  $gT^2S_h^-$  at  $a = (\sqrt{5} + 1)/2 + 0.2 = 1.818033 \dots$ . The intersection point  $z$  is an orbital point of  $1/5$ -BE.

From Definition 1 and Theorem 2, the branches of symmetry axes on which  $p/q$ -BE(BS) has a point are determined. The results are summarized as Property 3 (Yamaguchi and Tanikawa, 2009).

### Property 3.

- (i) If  $q$  and  $p$  are odd, then  $p/q$ -BE has one orbital point on  $S_g^+$  and another on  $S_h^-$ , while  $p/q$ -BS has one orbital point on  $S_g^-$  and another on  $S_h^+$ .
- (ii) If  $q$  is odd and  $p$  is even, then  $p/q$ -BE has one orbital point on  $S_g^+$  and another on  $S_h^+$ , while  $p/q$ -BS has one orbital point on  $S_g^-$  and another on  $S_h^-$ .
- (iii) If  $q$  is even and  $p$  is odd, then  $p/q$ -BE has one orbital point on  $S_g^+$  and another on  $S_g^-$ , while  $p/q$ -BS has one orbital point on  $S_h^+$  and another on  $S_h^-$ .

From now, we discuss the properties of involutions. Suppose that curve  $y = G(x)$  intersects  $S_g$  at  $z = (x, y)$ . Let  $\xi(z) = dG(x)/dx$  be the slope of the curve at  $z$ . Operating  $g$  to this curve, we obtain the image curve.

$$y = -G(x) - f(x). \quad (6)$$

Let  $\xi_g(z) = dy/dx$  be the slope of the image curve at  $z$ . We obtain the relation

$$\xi_g(z) = -\xi(z) - f'(x) \quad (7)$$

where  $f'(x) = df(x)/dx$ . There are two situations in which  $\xi_g(z)$  and  $\xi(z)$  coincide at  $z \in S_g$ . In the first case, both  $\xi_g(z)$  and  $\xi(z)$  diverge. In the second case, the relations  $\xi(z) = \xi_g(z) = -f'(x)/2$  hold where  $-f'(x)/2$  is the slope of  $S_g$  at  $z$ .

Next, suppose that the curve represented by  $y = H(x)$  intersects  $S_h$  at  $w = (x, 0)$ . Let  $\eta(w) = dH(x)/dx$  be the slope of the curve at  $w$ . Operating  $h$  to this curve, we have  $hH(x)$ .

$$y = -H(x - y). \quad (8)$$

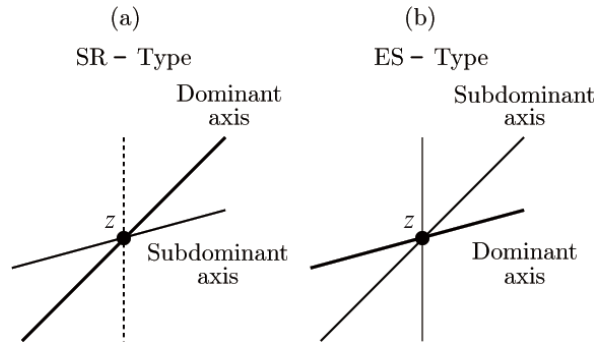


Fig. 3. Two types of the intersection of the dominant axis and the subdominant axis. (a) SR-Type (abbreviation of saddle with reflection) where  $\xi(z) < \xi_D(z)$  holds. (b) ES-Type (abbreviation of elliptic or saddle) where  $\xi(z) > \xi_D(z)$  holds. This type includes the situation that the slope of the subdominant axis diverges.

Let  $\eta_h(w) = dy/dx$  be the slope of  $hH(x)$  at  $w$ . We obtain the relation

$$\eta_h(w) = \frac{\eta(w)}{\eta(w) - 1}. \quad (9)$$

There exists the situation that the function  $H(x)$  and its image  $hH(x)$  are tangent at  $w \in S_h$ . At the tangency situation, the following relations hold.

$$\eta(w) = \eta_h(w) = 0 \text{ or } \eta(w) = \eta_h(w) = 2. \quad (10)$$

### 2.3 Involutions and symmetry axes for $T^q$

Mapping  $T^q$  is also reversible. In fact, it can be represented by a product of two involutions. Here let us define the subdominant axis which makes a pair with the dominant axis.

**Definition 4 (Subdominant axis).** Mapping  $T^q$  ( $q \geq 1$ ) is represented as follows.

$$T^q = T^{q-1}h \circ g. \quad (11)$$

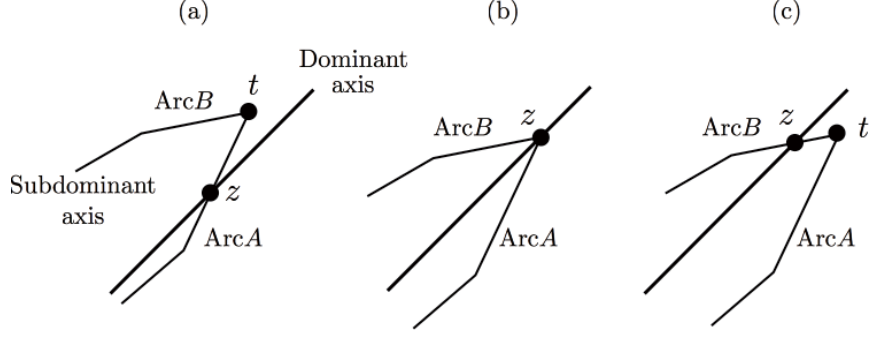


Fig. 4. (a) At  $a < a_c^{\text{ex}}(p/q)$ , ArcA of the subdominant axis and the dominant axis  $S_g^+$  intersect at  $z$ . The intersection is of ES-Type. (b) At  $a = a_c^{\text{ex}}(p/q)$ , the relation  $t = z \in S_g^+$  holds. This situation represents the situation of the exchange bifurcation. (c) At  $a > a_c^{\text{ex}}(p/q)$ , ArcB of the subdominant axis and the dominant axis  $S_g^+$  intersect at  $z$ . The intersection is of SR-Type.

Here,  $T^{q-1}h$  is an involution. The corresponding symmetry axis is named the subdominant axis, and is denoted by  $S_{T^{q-1}h}$ .

We have two representations for the subdominant axis depending on the parity of  $q$ .

$$S_{T^{q-1}h} = T^k S_h \text{ for } q = 2k + 1 \ (k \geq 1), \quad (12)$$

$$S_{T^{q-1}h} = T^k S_g \text{ for } q = 2k \ (k \geq 1). \quad (13)$$

Operating  $g$  on the subdominant axis is equivalent to operating  $T^{-q}$  on it. Suppose that the dominant and subdominant axes intersect at point  $z = (x, y)$  other than  $Q$ . Let the slopes of the subdominant axis and its image  $gS_{T^{q-1}h}$  at  $z$  be  $\xi(z)$  and  $\xi_g(z)$ . For them, Eq. (7) holds.

Let us study the relation between  $\xi(z)$  and  $\xi_g(z)$  for  $q = 3$ . In this case, the subdominant axis is  $TS_h^-$ . Point  $z$  is the intersection of  $S_g^+$  and  $TS_h^-$ , and is an orbital point of the 1/3-BE. We put  $a = 3.3 > a_c(1/3) = 4 \sin^2(\pi/3) = 3$ . In Fig. 2(a), the relation of  $TS_h^-$  and  $gTS_h^-$  is displayed. For a point  $u_0 \in TS_h^-$ , we have  $u_1 = gu_0 = T^{-3}u_0$  and  $u_0 = gu_1 = T^{-3}u_1$ . Thus,  $u_0$  and  $u_1$  are the orbital points of the daughter periodic orbit appearing through period doubling bifurcation of  $z$ . The period of the daughter orbit is 6. The slope  $\xi(z)$  of the subdominant axis and the slope  $\xi_g(z)$  of  $gTS_h^-$  satisfy the relation  $\xi(z) < \xi_g(z)$ .

Next, we consider the case  $q = 5$  (Fig. 2(b)). The subdominant axis  $T^2S_h^-$  and the dominant axis intersect at the orbital point  $z$  of 1/5-BE. We see  $T^2S_h^-$  and its image  $gT^2S_h^-$  in the figure. There are no other intersection points around  $z$ . Slopes  $\xi(z)$  and  $\xi_g(z)$  of the subdominant axis and of  $gT^2S_h^-$  satisfy relation  $\xi(z) > \xi_g(z)$ . This means that  $z$  is an elliptic point with complex eigenvalues, or a saddle point. From the results mentioned above, we obtain Proposition 5, which talks about a new geometric method to determine the appearance of period doubling bifurcation.

**Proposition 5.** Suppose that subdominant axis  $S_{T^{q-1}h}$  and its image  $gS_{T^{q-1}h}$  intersect at  $z$ . Let  $\xi_D(z)$ ,  $\xi(z)$  and  $\xi_g(z)$ , respectively, be the slopes at  $z$  of the dominant axis, the subdominant axis and its image.

(i) Relations  $\xi(z) > \xi_D(z) > \xi_g(z)$  hold before period doubling bifurcation of  $z$ .

(ii) Both  $\xi(z)$  and  $\xi_g(z)$  diverge at the critical situation of period doubling bifurcation of  $z$ .

(iii) Relations  $\xi(z) < \xi_D(z) < \xi_g(z)$  hold after period doubling bifurcation of  $z$ .

We classify the intersections of the dominant and subdominant axes into two types (see Fig. 3).

**Classification 6.** Let  $z = (x, y)$  be the intersection point of the dominant and subdominant axes, and  $\xi_D(x)$  and  $\xi(x)$  be their slopes at  $z$ .

(i) SR-Type: relation  $\xi(x) < \xi_D(x)$  holds, and  $z$  is a saddle periodic point with reflection. Abbreviation SR represents saddle with reflection.

(ii) ES-Type: relation  $\xi(x) > \xi_D(x)$  holds, and  $z$  is an elliptic periodic point with complex eigenvalues or a saddle periodic point. This type includes the case that  $\xi(x)$  diverges. Abbreviation ES represents elliptic or saddle.

We define the exchange bifurcation.

**Definition 7 (Exchange bifurcation).** Let  $t$  be one of the break points of the piecewise linear subdominant axis, and  $z$  be the intersection point of the dominant axis and the subdominant axis. Let  $p/q$  be the rotation number of the orbit of  $z$ . Suppose that ArcA and ArcB of the subdominant axis is connected at point  $t$ . Suppose there exists a  $a_c^{\text{ex}}(p/q)$  such that, for  $a < a_c^{\text{ex}}(p/q)$ , ArcA intersects the dominant axis at  $z$  with  $t$  above  $S_g^+$  (Fig. 4(a)), at  $a = a_c^{\text{ex}}(p/q)$ ,  $t (= z)$  is on  $S_g^+$  (Fig. 4(b)), and for  $a > a_c^{\text{ex}}(p/q)$ , ArcB intersects the dominant axis at  $z$  with  $t$  below  $S_g^+$  (Fig. 4(c)). The stability of  $z$  in  $a < a_c^{\text{ex}}(p/q)$  differs from that in  $a > a_c^{\text{ex}}(p/q)$ . We name this bifurcation the exchange bifurcation. If the exchange bifurcation coincides with the rotation bifurcation, we treat it as the rotation bifurcation.

Finally, we represent  $T^q$  as  $T^q = h \circ gT^{q-1}$ . We denote the invariant set of  $gT^{q-1}$  by  $S_{gT^{q-1}}$ . We give the representations for  $S_{gT^{q-1}}$ .

$$S_{gT^{q-1}} = T^{-k} S_g \text{ for } q = 2k + 1 \ (k \geq 1), \quad (14)$$

$$S_{gT^{q-1}} = T^{-k} S_h \text{ for } q = 2k \ (k \geq 1). \quad (15)$$

Operating  $h$  on  $S_{gT^{q-1}}$  is equivalent to operating  $T^q$  on  $S_{gT^{q-1}}$ .

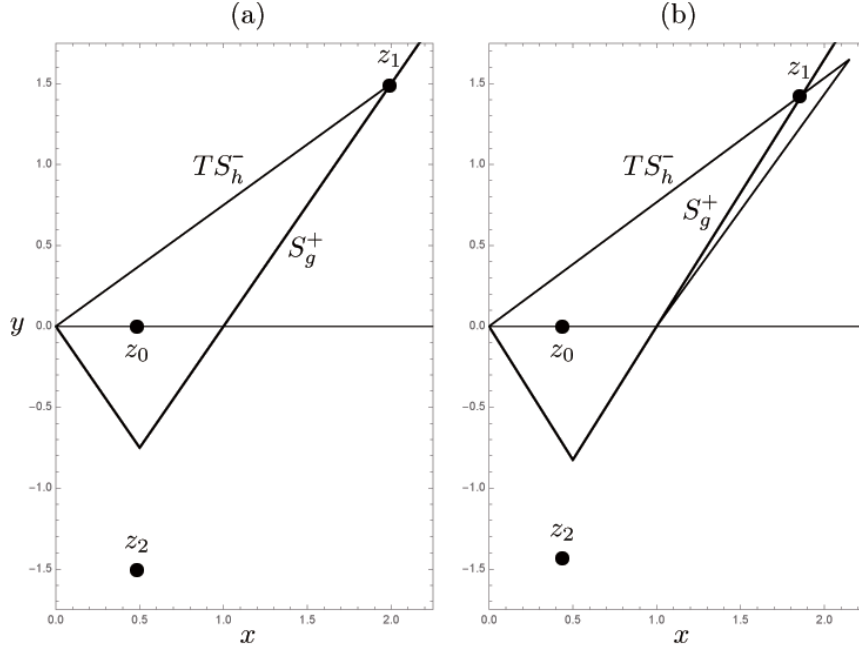


Fig. 5. Bifurcations of 1/3-BE. (a)  $a = a_c(1/3) = 3$ . The situation at which the rotation bifurcation occurs. (b)  $a = 3.3$ . At  $a > a_c(1/3)$ , the intersection point is of SR-Type and is a saddle with reflection.

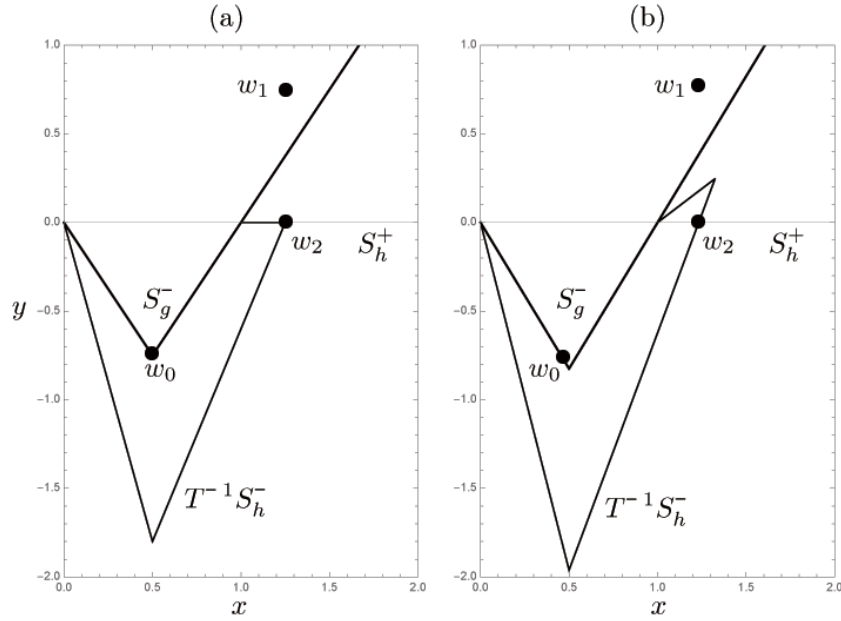


Fig. 6. Bifurcations of 1/3-BE. The relation between  $T^{-1}S_h^-$  and  $S_h^+$  is displayed. (a)  $a = a_c(1/3) = 3$ . The situation at which the rotation bifurcation occurs. (b)  $a = 3.3$ .

#### 2.4 Linear stability analysis

If point  $z = (x, y)$  is in  $x < 1/2$ , the coefficient matrix  $m_0$  of the linearized system at  $z$  is given by

$$m_0 = \begin{pmatrix} 1 & a \\ 1 & 1+a \end{pmatrix}, \quad (16)$$

while if  $z = (x, y)$  is in  $x > 1/2$ , the matrix  $m_1$  at  $z$  is given by

$$m_1 = \begin{pmatrix} 1 & -a \\ 1 & 1-a \end{pmatrix}. \quad (17)$$

Take a periodic orbit  $\{z_0 = Tz_{q-1}, z_1 = Tz_0, \dots, z_{q-1} = Tz_{q-2}\}$  of period- $q$  ( $\geq 2$ ) and suppose that  $z_k$  ( $0 \leq k \leq q-2$ ) be in  $x < 1/2$ , and  $z_{q-1}$  in  $x > 1/2$ . The stability of this orbit is determined by the eigenvalues of matrix  $m = m_1 m_0^{q-1}$ . Let  $r(a) = \text{Tr } m$  (Trace of  $m$ ). We obtain the equation to determine the eigenvalue  $\lambda$ .

$$\lambda^2 - r(a)\lambda + 1 = 0. \quad (18)$$

Using  $r(a)$ , the stability of periodic orbits is classified into three types as in Classification 8.

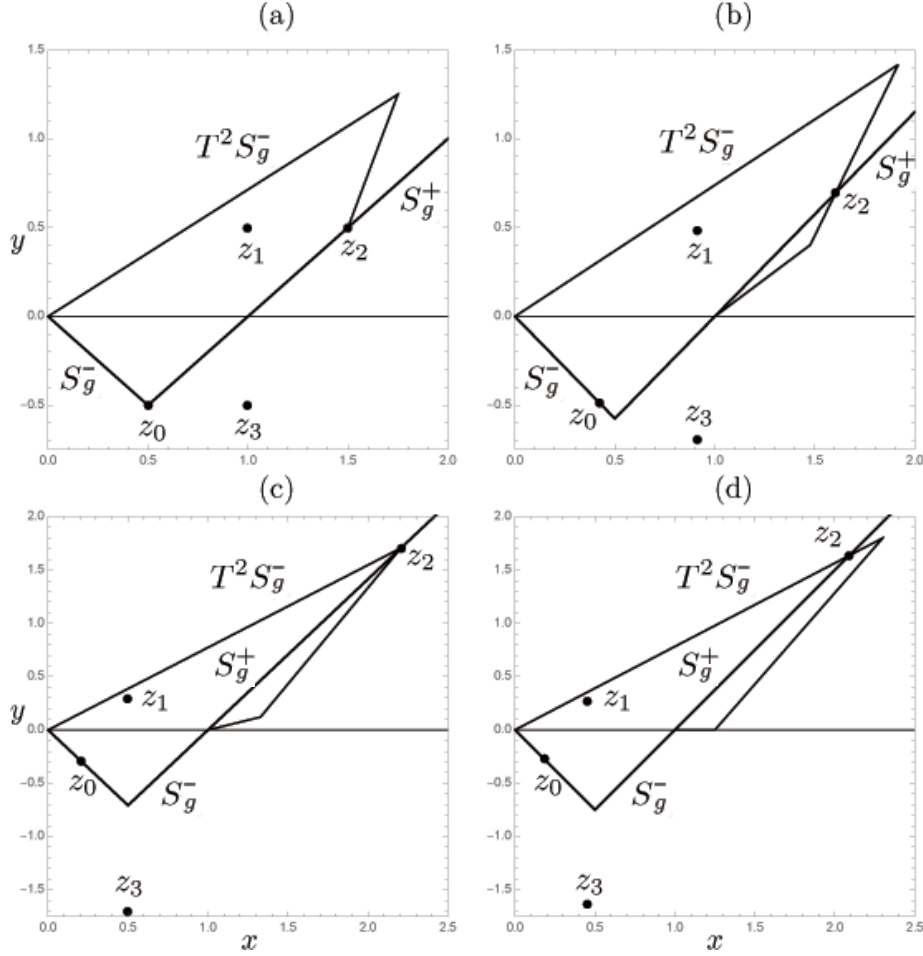


Fig. 7. Bifurcations of 1/4-BE. (a)  $a = a_c(1/4) = 2$ . The critical point at which the rotation bifurcation occurs. (b)  $a = 2.3$ . At  $a > a_c(1/4)$ , the intersection type is ES-Type and 1/4-BE is the saddle orbit. (c)  $a = 2\sqrt{2}$ . The critical point at which the first exchange bifurcation occurs. (d)  $a = 3$ . The intersection type is SR-Type and 1/4-BE is the saddle with reflection.

### Classification 8.

- (i)  $r(a) > 2$ : the periodic orbit is of saddle type.
- (ii)  $|r(a)| \leq 2$ : the periodic orbit is of elliptic type with complex eigenvalues.
- (iii)  $r(a) < -2$ : the periodic orbit is of saddle type with reflection.

Note that the residue  $R$  defined by Greene (Greene,1979) is  $R = (2 - r(a))/4$ .

### 3. Analysis of Bifurcations

In the piecewise linear maps, the periodic point is frequently on the break point of the piecewise linear symmetry axis. In these timings, bifurcations take place discontinuously. In this section, as typical examples, we study the bifurcations of 1/3-BE (BS), 1/4-BE (BS) and 1/5-BE (BS). We hope these examples exhaust the types of bifurcation appearing in the Lozi map.

#### 3.1 Bifurcations for the periodic orbits with rotation number 1/3

First, we study the bifurcations of 1/3-BE. In this case, the subdominant axis is  $TS_h^-$ . At  $a = a_c(1/3) = 4 \sin^2(\pi/3) = 3$ , one piece of  $TS_h^-$  overlaps the dominant axis  $S_g^+$  (Fig. 5(a)). Every point of  $\text{Arc}[Q, z_1]_{S_g^+}$  is periodic with period-3. At the situation of the rotation bifurcation,

the slope of the subdominant axis agrees with that of the dominant axis ( $a/2 = 3/2$ ).

At  $a > 3$ , there exists intersection point  $z_1$  of  $TS_h^-$  and  $S_g^+$  (Fig. 5(b)) where  $z_1$  is of SR-Type. Thus, 1/3-BE is a saddle with reflection for  $a > 3$ . This means that there exists a daughter periodic orbit with period-6 appearing through period doubling bifurcation of 1/3-BE (see Fig. 2(a)). The rotation bifurcation, period doubling bifurcation and exchange bifurcation occur at the same parameter  $a = 3$ .

By Eq. (18), we can confirm the stability of 1/3-BE. Just after the rotation bifurcation,  $z_0$  and  $z_2$  are in  $x < 1/2$ , and  $z_1$  in  $x > 1/2$  (see Fig. 5(b)), from which we obtain  $m = m_0^2 m_1$  and

$$r(a) = -a^3 - 2a^2 + 3a + 2. \quad (19)$$

Since  $r(a) < r(3) = -34 < -2$  for  $a > 3$ , two eigenvalues  $\lambda_{\pm}$  of Eq. (19) satisfy relations  $\lambda_- < -1 < \lambda_+ < 0$  ( $\lambda_+ = 1/\lambda_-$ ). Thus, 1/3-BE is a saddle with reflection.

Next, we study the stability of 1/3-BE. The situation at  $a = 3$  is displayed in Fig. 6(a). The piece of  $T^{-1}S_h^-$  overlaps  $S_g^+$ , and the  $x$ -coordinate of  $w_0$  is  $x = 1/2$ . Just after the rotation bifurcation (see Fig. 6(b)),  $w_0$  is in  $x < 1/2$ , and  $w_1$  and  $w_2$  in  $x > 1$ . Since  $w_2 = gw_1$  holds, the

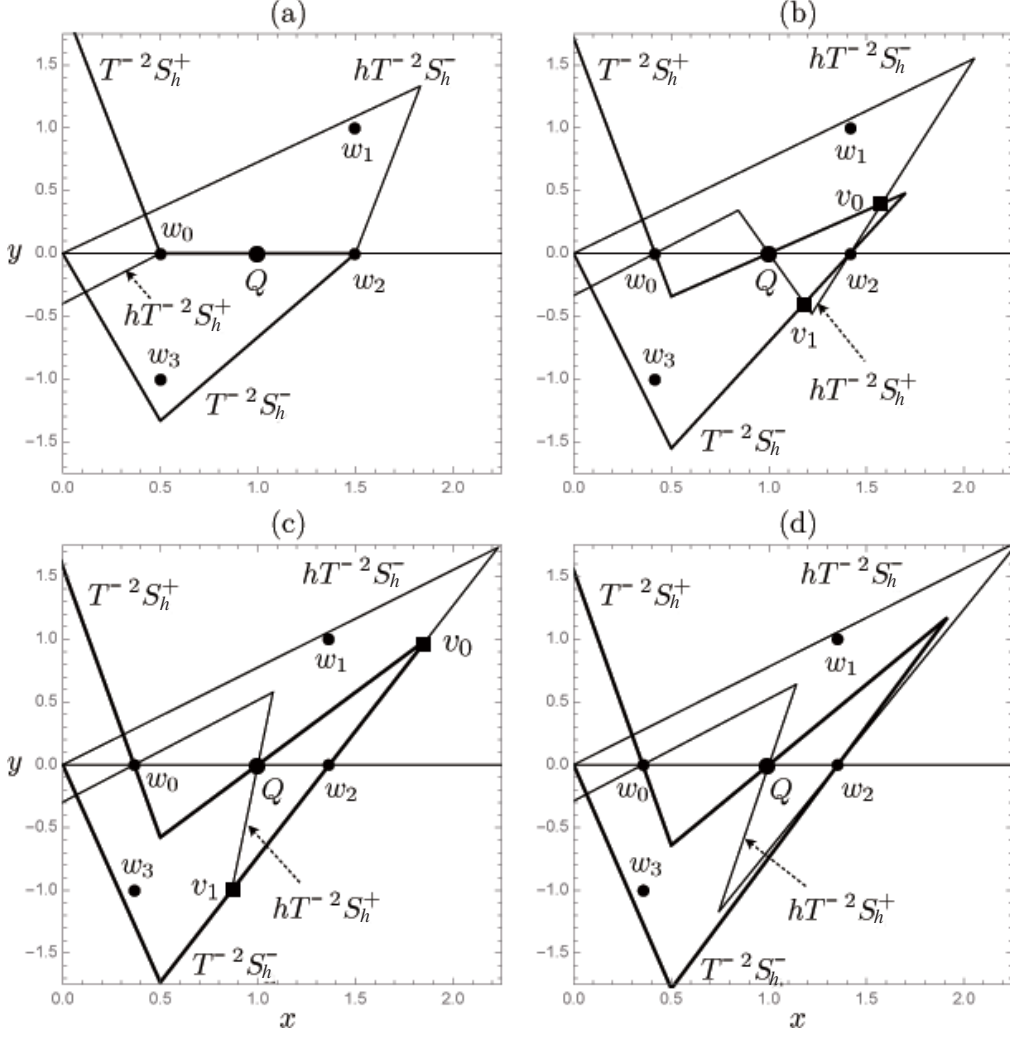


Fig. 8. Bifurcations of 1/4-BS. (a)  $a = a_c(1/4) = 2$ . The critical point at which the rotation bifurcation occurs. (b)  $a = 2.4$ . Filled squares represent the daughter periodic points  $v_0$  and  $v_1$  with period-8 appeared from  $w_2$ . (c)  $a = 2.732050\dots$ . The critical point at which the inverse period doubling bifurcation occurs and the daughter periodic points disappear. (d)  $a = 2\sqrt{2}$ . The critical point at which the exchange bifurcation occurs.

$x$ -coordinates for  $w_1$  and  $w_2$  are the same. By the existence of  $Q$ ,  $w_2$  does not move into  $x < 1$ . Thus, for  $a > 3$ ,  $w_1$  and  $w_2$  are in  $x > 1$ . From the configuration mentioned above, we obtain  $m = m_0 m_1^2$  and

$$r(a) = a^3 - 2a^2 - 3a + 2. \quad (20)$$

Since  $r(a) > r(3) = 2$  for  $a > 3$ , two eigenvalues  $\lambda_{\pm}$  satisfy relations  $0 < \lambda_- < 1 < \lambda_+$ . Thus, 1/3-BS is a saddle. It is noted that the name BE (BS) is consistent with its stability. The dominant axis theorem holds for 1/3-BE.

### 3.2 Bifurcations for the periodic orbit with rotation number 1/4

Here we study the bifurcations for the periodic orbit with rotation number 1/4. In this case, the subdominant axis is  $T^2 S_g^-$ . At  $a = a_c(1/4) = 4 \sin^2(\pi/4) = 2$ , a piece of the subdominant axis overlaps dominant axis  $S_g^+$ . Every point of  $\text{Arc}[Q, z_2]_{S_g^+}$  in Fig. 7(a) is periodic with period-4. At  $a > 2$ , there exists intersection point  $z_2$  of  $T^2 S_g^-$  and  $S_g^+$  (Fig. 7(b)) where  $z_2$  is of ES-Type. Just after the rotation bifurcation,  $z_0$  is in  $x < 1/2$  and the other three points are in  $x > 1/2$ . So, we obtain  $m = m_0 m_1^3$  and

$$r(a) = -a^4 + 4a^3 - 8a + 2. \quad (21)$$

1/4-BE is of saddle type just after the rotation bifurcation since  $r(2 + \epsilon) = 2 + 8\epsilon - 4\epsilon^3 - \epsilon^4 > 2$  for  $0 < \epsilon \ll 1$ .

From Property 3, we have to confirm the stability of 1/4-BS which has the orbital points on  $S_h^+$  and on  $S_h^-$ . This situation at the rotation bifurcation is displayed in Fig. 8(a). After the situation of the rotation bifurcation (see Figs. 8(b)–(d)), the orbital points  $w_0$  and  $w_3$  are in  $x < 1/2$ , and  $w_1$  and  $w_2$  in  $x > 1/2$ . Therefore, we obtain  $m = m_0^2 m_1^2$  and

$$r(a) = a^4 - 8a^2 + 2. \quad (22)$$

Since  $r(2) = -14 < -2$  and  $r(a) > r(2)$  for  $a > 2$ , 1/4-BS is a saddle with reflection just after the rotation bifurcation. 1/4-BS undergoes the inverse period doubling bifurcation at  $a = 2.732050\dots$  which is the solution of  $r(a) = -2$ , and it becomes elliptic with complex eigenvalues.

In Figs. 8(a)–(d), thick lines represent  $T^{-2} S_h^{\pm}$ , and thin ones  $hT^{-2} S_h^{\pm}$ . In Figs. 8(a) and (c), there exists the overlap interval of  $T^{-2} S_h^{\pm}$  and  $hT^{-2} S_h^{\pm}$ . The slope of the overlap interval including  $Q$  in Fig. 8(a) is zero and that including  $w_2$  in Fig. 8(c) is 2 (see Eq. (10)).

In Fig. 8(b), two intersection points  $v_0$  and  $v_1$  of thick

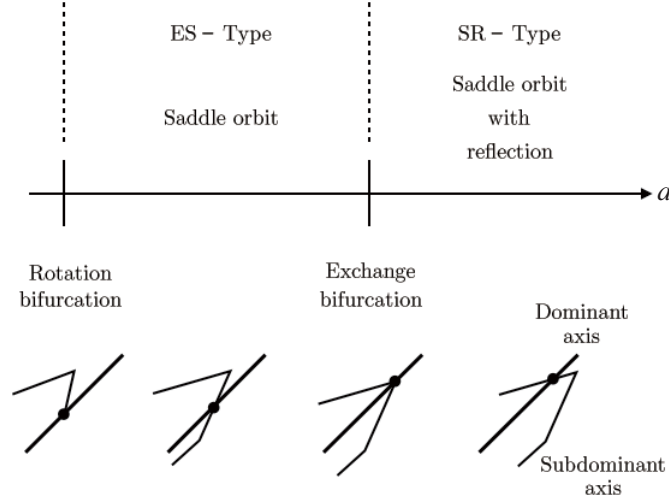


Fig. 9. Summary of the bifurcations for 1/4-BE.

and thin arcs exist in the vicinity of  $w_2$ . We remark that  $v_1 = hv_0$ ,  $v_1 = T^4v_0$  and  $v_0 = T^4v_1$ . Thus, the period of these daughter points is 8. The points  $v_0$  and  $v_1$  bifurcate from  $w_2$ . The inverse period doubling bifurcation of  $w_2$  happens in the passage from Fig. 8(b) to Fig. 8(c). The daughter periodic orbit with period-8 appearing at  $a = 2$  is absorbed into 1/4-BE at  $a = 2.732050\dots$ . This is the meaning of the inverse period doubling bifurcation.

The equiperiod bifurcation occurs at  $a = 2\sqrt{2}$  which is the solution of  $r(a) = 2$  (see Eq. (22)). This critical value is equal to that of the exchange bifurcation. For 1/4-BE and 1/4-BE, the stability exchange occurs at  $a = 2\sqrt{2}$  (Tanikawa and Yamaguchi, 2001). As a result, at  $a > 2\sqrt{2}$ , 1/4-BE is of elliptic type (see Fig. 7(d)) and 1/4-BE is of saddle type. The inconsistency of names for 1/4-BE and 1/4-BE is dissolved.

Here, we discuss the exchange of stabilities at  $a = 2\sqrt{2}$  (see Figs. 7(c) and 8(d)). Two daughter saddle periodic orbits are born from 1/4-BE, and two daughter elliptic periodic orbits are born from 1/4-BE. These four periodic orbits are non-symmetric. At  $a \geq a_c^{\text{SH}}$ , the horseshoe exists in the Lozi map. In the horseshoe, there is no non-symmetric periodic orbits with period-4 (see Appendix B). This means the disappearance of non-symmetric periodic orbits at some stage.

For 1/4-BE, the exchange bifurcation occurs once. The bifurcations of 1/4-BE are summarized in Fig. 9. The dominant axis theorem does not hold for 1/4-BE.

### 3.3 Bifurcations for the periodic orbit with rotation number 1/5

We study the bifurcations for 1/5-BE. In this case, the subdominant axis is  $T^2S_h^-$ . At  $a = a_c(1/5) = 4\sin^2(\pi/5) = (5 - \sqrt{5})/2$ , a piece of the subdominant axis overlaps dominant axis  $S_g^+$  (Fig. 10(a)). Every point of  $\text{Arc}[Q, z_2]_{S_g^+}$  in Fig. 10(a) is periodic with period-5. At  $a > a_c(1/5)$ , there exists the intersection point  $z_2$  of  $T^2S_h^-$  and  $S_g^+$  (Fig. 10(b)). Point  $z_2$  is of SR-Type. This means that 1/5-BE is a saddle with reflection. This fact implies that the period doubling bifurcation of 1/5-BE also happens at  $a = a_c(1/5)$  and the daughter periodic orbit with period-

10 exists around 1/5-BE.

The second break point (counting from zero at Q) in the subdominant axis stays above the dominant axis and it approaches the dominant axis as  $a$  increases. At  $a = (\sqrt{5} + 1)/2$ , the slope of the piece of subdominant axis which intersects the dominant axis at  $z_2$  diverges (see Fig. 10(c)). In this case,  $z_0$  and  $z_4$  are in  $x < 1/2$ , and the other points are in  $x > 1/2$ . Then, we obtain  $m = m_0^2m_1^3$  and

$$r(a) = -a^5 + 2a^4 + 9a^3 - 14a^2 - 5a + 2. \quad (23)$$

The critical value is the root of  $r(a) + 2 = -(a^2 - a - 1)(a^3 - a^2 - 9a + 4) = 0$ .

At  $a = (\sqrt{5} + 1)/2$ , the inverse period doubling bifurcation occurs and mother point  $z_2$  absorbs the two daughter periodic points. Just after the inverse period doubling bifurcation, mother point  $z_2$  is elliptic with complex eigenvalues, and the intersection of the dominant and subdominant axes changes to ES-Type.

Next, at  $a = 1.791287\dots$ , the mother point undergoes the equiperiod bifurcation and two daughter periodic points appear (see Fig. 10(d)). The critical value is the root of  $r(a) = 2$ . The period of the mother orbit and those of the daughter orbits are the same. The daughter periodic orbits are non-symmetric and thus are not displayed in Fig. 10(d).

Finally, the exchange bifurcation of  $z_2$  occurs at  $a = (\sqrt{21} + 1)/2$  (see Fig. 10(e)). At  $a > (\sqrt{21} + 1)/2$ , the intersection of the dominant and subdominant axes is of SR-Type (see Fig. 10(f)). Thus, the mother orbit is a saddle with reflection.

We explain how to derive  $a = (\sqrt{21} + 1)/2$ . The image of  $y = 0$  is  $y = ax/(a + 1)$ . The image of point  $(1/2, a/(2a + 2))$  on  $y = ax/(a + 1)$  is a break point represented as

$$\left( \frac{a^2 + 3a + 1}{2a + 2}, \frac{a(a + 2)}{2a + 2} \right). \quad (24)$$

By the condition that the break point is on  $S_g^+$ , we obtain

$$a^2 - a - 5 = 0. \quad (25)$$

The root of this equation gives the critical value.

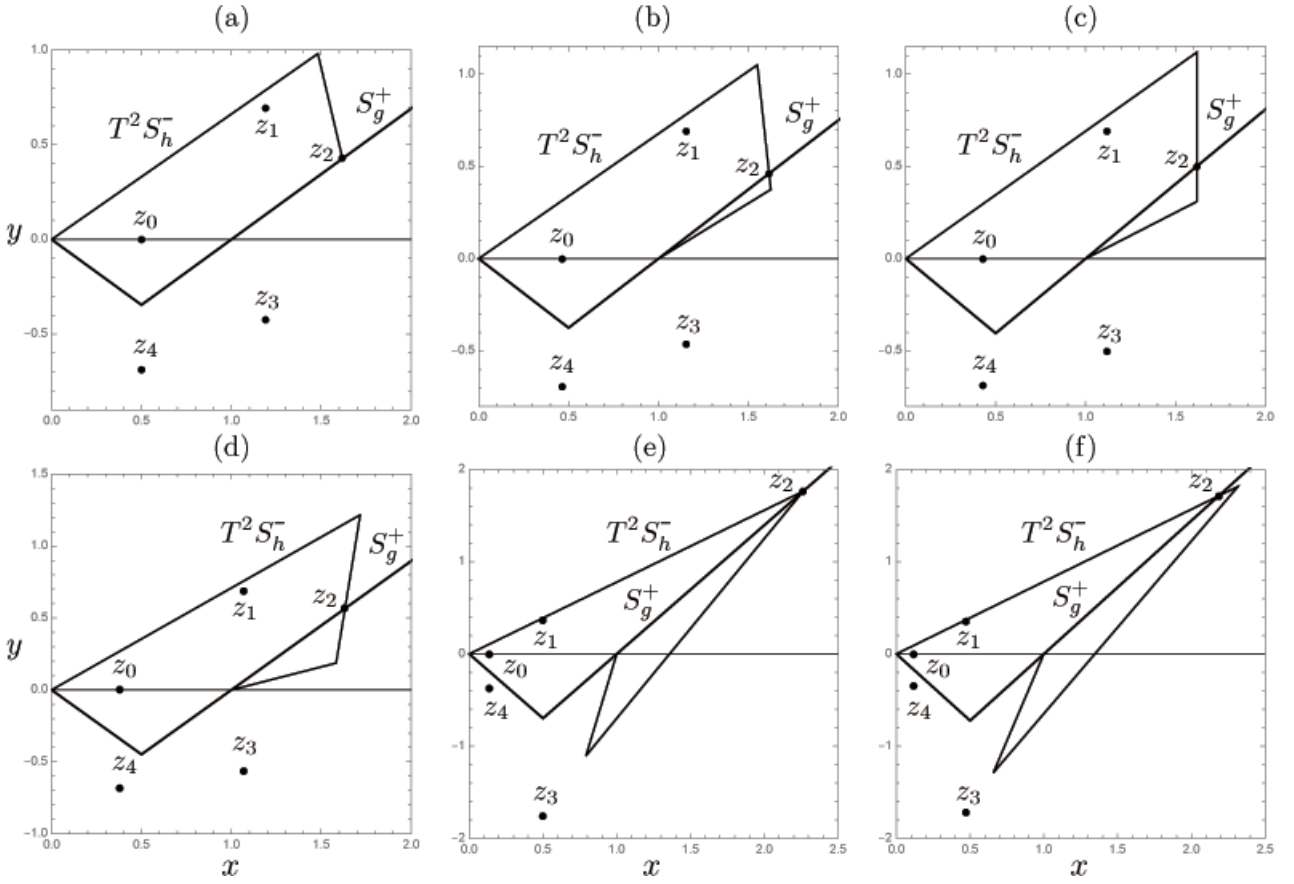


Fig. 10. Bifurcations of 1/5-BE. (a)  $a = 4 \sin^2(\pi/5)$ . The critical point at which the rotation bifurcation occurs. (b)  $a = 1.5$ . The intersection is of SR-Type, and 1/5-BE is a saddle with reflection. (c)  $a = (\sqrt{5} + 1)/2$ . The critical point at which the inverse period doubling bifurcation occurs. (d)  $a = 1.791287 \dots$ . The critical point at which the equiperiod bifurcation occurs. The intersection is of ES-Type. (e)  $a = (\sqrt{21} + 1)/2$ . The critical situation at which the first exchange bifurcation occurs. (f)  $a = (\sqrt{21} + 1)/2 + 0.1$ . The intersection is of SR-Type, and 1/5-BE is a saddle with reflection.

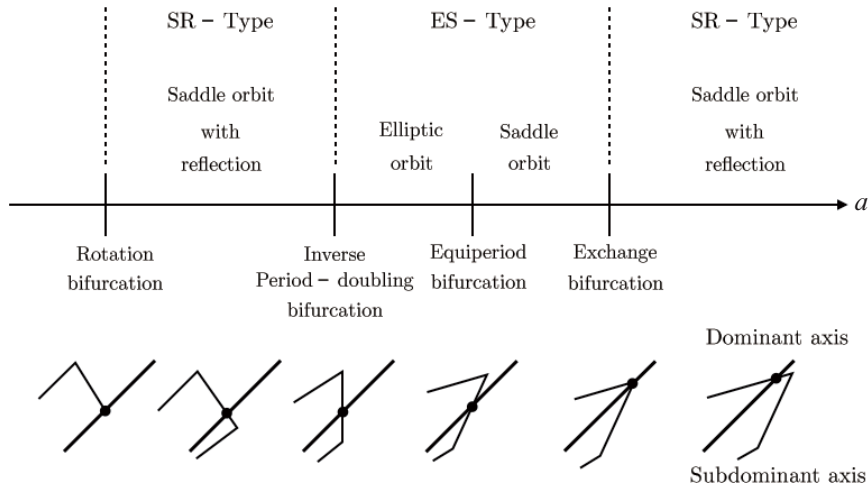


Fig. 11. Summary of the bifurcations for 1/5-BE.

The period doubling bifurcation also occurs at  $a = (\sqrt{21} + 1)/2$  and the daughter periodic orbit with period-10 appears. We remark that two non-symmetric periodic orbits disappear at  $a = (\sqrt{21} + 1)/2$ . This is derived from the fact that there is no non-symmetric periodic orbits with period-5 in the horseshoe (see Appendix B). The bifurcations of 1/5-BE are summarized in Fig.11. The dominant

axis theorem does not hold for 1/5-BE.

We comment on 1/5-BE. Just after the rotation bifurcation, this orbit is of saddle type. This orbit also experiences the bifurcations, and it becomes of saddle type after the exchange bifurcation. Just after the rotation bifurcation and after the exchange bifurcation, the name of BE (BS) is consistent with its stability.

#### 4. A New Theorem

If we increase the number of iterations, the number of break points of the image of the subdominant axis increases. Thus, the number of times that the exchange bifurcations occur also increases. Let us define the critical value  $a_c^{\text{le}}(p/q)$  at which the last exchange bifurcation occurs.

##### Definition 9 (Last exchange bifurcation).

- (i) In the case where the exchange bifurcation takes place plural times, let  $a_c^{\text{le}}(p/q)$  be the last critical value for which the exchange bifurcation takes place.
- (ii) In the case where the exchange bifurcation takes place only once at  $a = a_c^{\text{ex}}(p/q)$ , we let  $a_c^{\text{le}}(p/q) = a_c^{\text{ex}}(p/q)$ .
- (iii) If the situation of the last exchange bifurcation is that of the rotation bifurcation, we let  $a_c^{\text{le}}(p/q) = a_c(p/q)$ .

We remark that Fig. 7(c) is the example of Definition 9(ii) and Fig. 5(a) is that of Definition 9(iii).

Next, we prove Proposition 10 which determines the intersection type of  $S_g^+$  and  $S_{T^{q-1}h}$  after the last exchange bifurcation.

**Proposition 10.** At  $a > a_c^{\text{le}}(p/q)$ , the intersection of  $S_g^+$  and  $S_{T^{q-1}h}$  is of SR-Type.

*Proof.* At the situation of the last exchange bifurcation, let  $z_k$  be the intersection point on  $S_g^+$ . This point is also the break point  $t$ . There is no break point in  $\text{Arc}[P, t]_{S_{T^{q-1}h}}$ . After the last exchange bifurcation, the break point  $t$  moves to the right region of  $S_g^+$ . In order that  $\text{Arc}[P, t]_{S_{T^{q-1}h}}$  intersects  $S_g^+$  at  $z_k$ , the slope of  $\text{Arc}[P, t]_{S_{T^{q-1}h}}$  should be less than that of  $S_g^+$  (see Figs. 5(b), 7(d), and 10(f)). This implies the claim. (Q.E.D.)

If the equiperiod bifurcation does not occur at the situation of ES-Type, the periodic orbit is of elliptic type with complex eigenvalues. For this case, the dominant axis theorem holds. The typical example is 1/3-BE.

For 1/5-BE, just after the rotation bifurcation, the periodic orbit is of elliptic type with complex eigenvalues. But, the equiperiod bifurcation occurs and the periodic orbit becomes the saddle orbit. For 1/4-BE, just after the rotation bifurcation, the periodic orbit is the saddle. The exchange of the stability exchange between 1/4-BE and 1/4-BS happens. Thus, the dominant axis theorem does not hold for 1/4-BE and 1/5-BE. These examples give the reason why the dominant axis theorem for  $p/q$ -BE is not necessarily true. Therefore, we obtain Result 11.

**Result 11.** There are two origins that the dominant axis theorem does not hold.

- (i) Occurrence of the equiperiod bifurcation.
- (ii) Occurrence of the stability exchange between  $p/q$ -BE and  $p/q$ -BS.

Finally, from Proposition 10, we obtain a new theorem (Theorem 12) which is the restricted version of Theorem 2.

**Theorem 12.** In the Lozi map, at  $a > a_c^{\text{le}}(p/q)$ , the  $p/q$ -BE with  $0 < p/q \leq 1/2$  has the orbital point on the dominant axis  $S_g^+$  and it is a saddle with reflection.

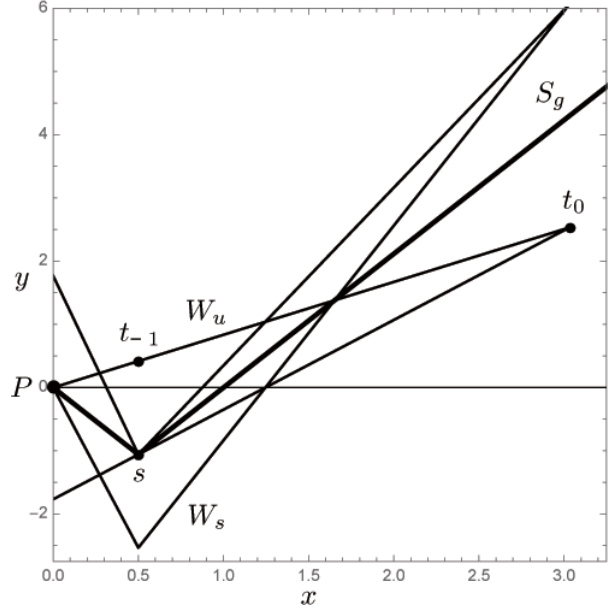


Fig. A.1. Completion of the horseshoe. At  $a = a_c^{\text{SH}} = 4.229981\dots$ , the stable manifold  $W_s$  and the unstable manifold  $W_u$  are tangent at  $s \in S_g$ . The break point  $t_0 = Tt_{-1}$  is the first turning point of the unstable manifold. The second turning point  $t_1$  is not displayed.

#### 5. Conclusion

We summarize our results.

- (1) Using the involutions for  $T^q$ , we give the geometric method to study the period doubling bifurcation.
- (2) We introduce two intersection types, ES-type and SR-Type. If ES-type appears,  $p/q$ -BE is a saddle orbit or an elliptic orbit with complex eigenvalues, while, if SR-Type appears,  $p/q$ -BE is a saddle with reflection.
- (3) We make clear the reason why the dominant axis theorem does not hold for the Lozi map, and obtain the new theorem instead of the dominant axis theorem.

#### Appendix A.

The initial arc of the unstable manifold  $W_u$  starting at  $P$  and extending to the upper-right direction is represented as

$$y = \xi_u(0)x \quad (\text{A.1})$$

where

$$\xi_u(0) = \frac{-a + \sqrt{a^2 + 4a}}{2}. \quad (\text{A.2})$$

The unstable manifold is piecewise linear. The second piece of  $W_u$  returns back close to  $P$  (see Fig. 1). We call this the lower branch.

Take a point  $t_{-1} = (1/2, \xi_u(0)/2)$  on  $W_u$ . Its image  $t_0 = Tt_{-1}$  is the first break and turning back point of  $W_u$ . The next image  $t_1 = Tt_0$  locates on the lower branch, and is the second turning point. However, it is in  $x < 0$  and  $y < 0$  and thus is not displayed in Fig. A.1. In Fig. 1 where the parameter value is smaller, the second and third turning points of the unstable manifold are observed in  $x > 0$ .

Using Eq. (1), we determine the positions of  $t_0$  and  $t_1$ .

$$t_0 = \left( \frac{\xi_u(0) + a + 1}{2}, \frac{\xi_u(0) + a}{2} \right), \quad (\text{A.3})$$

$$t_1 = \left( \frac{-a^2 - a(\xi_u(0) - 3) + 2\xi_u(0) + 1}{2}, \frac{-a^2 - a(\xi_u(0) - 2) + \xi_u(0)}{2} \right). \quad (\text{A.4})$$

The equation representing the lower branch is determined.

$$y = \alpha x + \beta, \quad (\text{A.5})$$

$$\alpha = \frac{a(a + \xi_u(0) - 1)}{a^2 + a(\xi_u(0) - 2) - \xi_u(0)}, \quad (\text{A.6})$$

$$\beta = \frac{-(2a^2 + \xi_u^2(0) + a(3\xi_u(0) - 1))}{2(a^2 + a(\xi_u(0) - 2) - \xi_u(0))}. \quad (\text{A.7})$$

In Fig. A.1, the unstable manifold and the stable manifold are tangent at  $s \in S_g$ . This implies the completion of the horseshoe. Using the condition that  $s = (1/2, -a/4) \in S_g$  locates on the lower branch represented by Eq. (A.5), we obtain the equation to determine the critical value at which the horseshoe completes.

$$-\frac{a}{4} = \frac{\alpha}{2} + \beta. \quad (\text{A.8})$$

After a long calculation, the simplified equation to determine the critical value is derived.

$$2a^3 - 8a^2 - a - 4 = 0. \quad (\text{A.9})$$

Here, Eq. (A.2) for  $\xi_u(0)$  is used. Solving this equation, we obtain the critical value  $a_c^{\text{SH}}$ .

$$a_c^{\text{SH}} = (8 + (800 - 30\sqrt{330})^{1/3} + (10(80 + 3\sqrt{330}))^{1/3})/6 = 4.229981 \dots \quad (\text{A.10})$$

## Appendix B.

In the horseshoe, orbits are coded uniquely by two symbols 0 and 1 (Gilmore and Lefranc, 2002; Yamaguchi and Tanikawa, 2016). The word of the minimum period for the periodic sequence is called a code. Let us consider period-4 and period-5 orbits.

For period-4, there exist three periodic orbits. Their codes are represented as follows.

$$0001, 0011, 0111.$$

Here, the cyclic permutation for codes is permitted. The first code represents 1/4-BE and the second one 1/4-BS.

These periodic orbits appear through rotation bifurcation of  $Q$ . The third code represents the daughter periodic orbit appearing through period doubling bifurcation of the period-2 orbit (1/2-BE) with code 01.

There exist six codes with period-5.

$$00001, 00011, 01101, 01111, 00101, 00111.$$

Here, the first code represents 1/5-BE, the second one 1/5-BS, the third one 2/5-BE, and the fourth one 2/5-BS. These periodic orbits appear through rotation bifurcation of  $Q$ . The last two codes represent the periodic orbits appearing through saddle-node bifurcation.

Let us consider the time-reversed code. For example, the time-reversal of  $s = 00101$  is  $s^{-1} = 10100$ . After operating cyclic permutation, 10100 is represented as 00101. Thus, the relation  $s = s^{-1}$  holds. If the code  $s$  satisfies  $s = s^{-1}$  after cyclic permutation, the code is said to be symmetric. If the code  $s$  is symmetric, the periodic orbit with code  $s$  is symmetric. All codes mentioned above are symmetric. Therefore, there are no non-symmetric periodic orbits with period-4 and 5 in the horseshoe. This implies that non-symmetric periodic orbits with period-4 or 5 disappear before the completion of horseshoe even if they appear through equiperiod bifurcation.

## References

- Birkhoff, D. G. (1966) *Dynamical Systems*, American Mathematical Society. Revised edition.
- Dulling, H. R., Meiss, J. D. and Sterling, D. (2005) Symbolic codes for rotational orbits, *SIAM J. Appl. Dyn. Sys.* **4**, 515–562.
- Elhadj, Z. (2013) *Lozi Map: Theory and Application*, CRC Press.
- Gilmore, R. and Lefranc, M. (2002) *The Topology of Chaos*, John Wiley & Sons.
- Greene, J. M. (1979) A method of computing the stochastic transition, *J. Math. Phys.* **20**, 1183–1201.
- Guckenheimer, J. and Holmes, P. (1983) *Nonlinear Oscillations, Dynamical Systems, and Bifurcations of Vector Fields*, Springer-Verlag.
- Hénon, M. (1976) A two-dimensional mapping with a strange attractor, *Comm. Math. Phys.* **50**, 69–77.
- Lozi, R. (1978) Un attracteur étrange du type attracteur de Hénon, *J. Physique (Paris)* **39** (Coll. C5), 9–10.
- MacKay, R. and Meiss, J. (1983) Linear stability of periodic orbits in Lagrangian systems, *Phys. Lett.* **98A**, 92–94.
- Tanikawa, K. and Yamaguchi, Y. (2001) Running homoclinic and periodic points in standard-like mappings, *Prog. Theor. Phys.* **105**, 399–407.
- Yamaguchi, Y. and Tanikawa, K. (2009) A new interpretation of the symbolic codes for the Hénon map, *Prog. Theor. Phys.* **122**, 569–609.
- Yamaguchi, Y. and Tanikawa, K. (2016) *Roads to the Horseshoe*, Kyoritsu Publication (in Japanese).